

## BICARBONATE-ACTIVATED HYDROGEN PEROXIDE IN PRESENCE OF $\text{CaCo}_{0.5}\text{Fe}_{0.5}\text{O}_3$ PEROVSKITE FOR HIGHLY EFFICIENT CARBAMAZEPINE DEGRADATION

This study aims to investigate the role of bicarbonate as a co-oxidant towards facile activation of hydrogen peroxide into reactive radicals during catalysis. A different set of bicarbonate to hydrogen peroxide dosage ratios ( $R = 0, 0.5, 1, 5, 10, 15, 20, 25,$  and  $\infty$ ) were varied in the presence of  $\text{CaCo}_{0.5}\text{Fe}_{0.5}\text{O}_3$  perovskite during catalysis to enhance the oxidative degradation of carbamazepine (CBZ) micropollutants. It was found that only 10-13% of CBZ was degraded in the presence of a single oxidant ( $R = 0$  and  $R = \infty$ ). Interestingly, 98% degradation of CBZ was achieved within 45 min of reaction at an  $R$ -value of 20. This improvement in CBZ degradation was contributed to the facile generation of reactive radicals ( $\cdot\text{OH}$  and  $\cdot\text{CO}_3^-$ ) due to the efficient redox cycle during catalysis. The degradation of CBZ in the bicarbonate-activated hydrogen peroxide- $\text{CaCo}_{0.5}\text{Fe}_{0.5}\text{O}_3$  system at  $R = 20$  agrees well with the Behnajady-Modirshahla-Ghanbery reaction kinetics model. These results provide new insights into the modulation of bicarbonate to hydrogen peroxide dosage ratio ( $R$ ) for efficient oxidative degradation of recalcitrant micropollutants facilitated by  $\text{CaCo}_{0.5}\text{Fe}_{0.5}\text{O}_3$  perovskite catalysts in the bicarbonate-activated hydrogen peroxide system.

*Keyword:* Perovskite; Bicarbonate-Activated Hydrogen Peroxide System; Micropollutants; Kinetics

### 1. Introduction

Carbamazepine (CBZ) is an anticonvulsant or anti-epileptic drug that attenuates activity in the brain and restores the normal balance of neural activity. CBZ is commonly used to treat various medical issues including epilepsy, nerve pain, and bipolar disorder. Wilkinson et al. [1] reported that CBZ was the most frequently detected active pharmaceutical component in water basin up to 62% of sampling sites within 104 countries worldwide due to its drug's efficacy compared to other active compounds. The most recent detection revealed that CBZ was detected in high concentrations of up to 132  $\mu\text{g/L}$  (132000  $\text{ng/L}$ ) in the wastewater treatment plant (WWTP) of northern Tunisia [2]. Due to its widespread occurrence, CBZ has been identified as an emerging recalcitrant organic micropollutant in the NORMAN list of emerging substances [3] worldwide and classified as an endocrine disrupting chemical by the US Environmental Protection Agency [4]. Hence, the removal of CBZ serves as a crucial issue in preventing its entrance into surface and groundwater resources due to its potential toxicity impacts [5,6].

Several methods have been utilized to remove CBZ from the wastewater plant, such as physicochemical, biological, and chemical treatments. The current conventional treatment approaches do not adequately remove CBZ from treated water. Conventional wastewater treatment processes are reported to be able in removing only 32-35% of trace pollutants, including CBZ, from wastewater [7]. Consequently, the remaining CBZ may enter surface water and potentially reach drinking water resources [8].

Based on these facts, advanced oxidative degradation is introduced as an alternative process for the treatment of pharmaceutical waste, such as oxidation, ozonation, and photocatalysis [9]. For instance, a recent review by Feijoo et al. [10] showed that advanced oxidation is more efficient than biological and physical treatments in degrading recalcitrant contaminant, including CBZ. In fact, Dai et al. [11] reported that chemical based advanced oxidation, particularly in Fenton process is the most promising technique for CBZ degradation among all reported advanced oxidation processes due to its high performance (up to 67.8% for CBZ removal) and simplicity of reaction

<sup>1</sup> CHEMICAL ENGINEERING STUDIES, COLLEGE OF ENGINEERING, UNIVERSITI TEKNOLOGI MARA, CAWANGAN PULAU PINANG, 13500 PERMATANG PAUH, PULAU PINANG, MALAYSIA

<sup>2</sup> HYBRID NANOMATERIALS, INTERFACES & SIMULATION (HYMFAST), CHEMICAL ENGINEERING STUDIES, COLLEGE OF ENGINEERING, UNIVERSITI TEKNOLOGI MARA, CAWANGAN PULAU PINANG, 13500 PERMATANG PAUH, PULAU PINANG, MALAYSIA

\* Corresponding author: [noraida709@uitm.edu.my](mailto:noraida709@uitm.edu.my)



process that ensures a safe and low-cost operation. Moreover, Sönmez et al. [12] demonstrated that Fenton process enable to remove CBZ, up to 99.77% at effective pH of reaction mixture less than 3.5. However, despite the outstanding performance of this process, the pitfalls of the  $\text{H}_2\text{O}_2$  activation into  $\cdot\text{OH}$  radicals are limited within the specific pH range of the solution (pH: 3-7) during catalysis [12,13]. The Fenton or electro-Fenton processes tend to become less effective at  $\text{pH} > 3$  due to the formation of  $\text{Fe}(\text{OH})^+$  complex ions, which are inactive in the conversion of  $\text{H}_2\text{O}_2$  to  $\cdot\text{OH}$  radicals [14].

To account for this problem, a simple yet economical and eco-friendly approach is introduced by incorporating bicarbonate as an activator to mediate the activation of  $\text{H}_2\text{O}_2$  during catalysis. This process is known as a bicarbonate-activated hydrogen peroxide (BAP) system. In the presence of a BAP system, the activation of  $\text{H}_2\text{O}_2$  can be operated at a wider pH range (i.e., neutral or slightly alkaline pH (pH 6-9)) that can efficiently generate  $\cdot\text{OH}$  radicals whilst prolonging the lifetime of the catalysts [15]. Such findings are supported by Jawad et al., that found enhanced oxidative degradation of methyl orange dye (99% removal) [16] and 4-chlorophenol (75% removal) [17] within 60 minutes in a BAP system, compared to single  $\text{H}_2\text{O}_2$  activation, which only exhibited rate of organic pollutant's degradation within the range of 10-15%.

Moreover, a recent study [18] has proven an excellent organic pollutants degradation efficiency with the help of cobalt (Co) substitution within the structure of perovskite catalyst. For instance, Co substitution on the B-site of  $\text{LaCo}_x\text{Fe}_{1-x}\text{O}_3$  perovskite catalyst exhibited a higher catalytic activity in degrading bisphenol A (BPA) by achieving a complete (100%) removal within 30 minutes at substituted Co loading of  $x = 0.5$  substitution. Meanwhile, the pristine  $\text{LaFeO}_3$  only exhibited 20% removal. Despite these promising results, comprehensive investigations into the catalytic activity of these perovskites in the presence of varying concentrations of bicarbonate-activated hydrogen peroxide (BAP) have yet to be explored. Additionally, in-depth understanding on the functional role of bicarbonate in modulating the redox cycle of heterogeneous catalysts during catalysis in the BAP system [16,17,19-22] have yet to be addressed.

Hence, this study aims to investigate the role of bicarbonate as a co-oxidizing agent that facilitates the activation of  $\text{H}_2\text{O}_2$  into reactive radicals during the degradation of CBZ in the BAP- $\text{CaCo}_{0.5}\text{Fe}_{0.5}\text{O}_3$  perovskite system. The catalytic activity of the  $\text{CaCo}_{0.5}\text{Fe}_{0.5}\text{O}_3$  perovskite catalyst in the BAP system to degrade CBZ was evaluated by modulating the ratio of bicarbonate to  $\text{H}_2\text{O}_2$  ( $R$ ). The analogous oxidative degradation was further analyzed using electrochemical impedance spectroscopy (EIS) analysis to probe in-depth understanding of the redox cycle during catalysis. The results of this work provide new insights into the functional role of bicarbonate in modulating redox cycle of active sites within the structure of perovskite catalyst to facilitate the activation of  $\text{H}_2\text{O}_2$  into reactive radicals during oxidative degradation of CBZ.

## 2. Methodology

### 2.1. Chemicals

All chemicals are used as received such as ethylenediaminetetraacetic acid disodium salt dehydrate solution (EDTA-2Na,  $\geq 99\%$ ), ammonium hydroxide ( $\text{NH}_4\text{OH}$ , 25%), calcium nitrate tetrahydrate ( $\text{Ca}(\text{NO}_3)_2 \cdot 4\text{H}_2\text{O}$ ,  $\geq 99\%$ ), citric acid monohydrate ( $\text{C}_6\text{H}_8\text{O}_7 \cdot \text{H}_2\text{O}$ ,  $\geq 99\%$ ), cobalt (II) chloride hexahydrate ( $\text{CoCl}_2 \cdot 6\text{H}_2\text{O}$ ,  $\geq 99\%$ ), iron (III) nitrate nonahydrate, ( $\text{Fe}(\text{NO}_3)_3(\text{H}_2\text{O})_9$ ,  $\geq 99\%$ ), hydrogen peroxide ( $\text{H}_2\text{O}_2$ , 30% wt./wt.) and carbamazepine ( $\text{C}_{15}\text{H}_{12}\text{N}_2\text{O}$ ).

### 2.2. Synthesis of $\text{CaCo}_{0.5}\text{Fe}_{0.5}\text{O}_3$ perovskite catalyst

$\text{CaCo}_{0.5}\text{Fe}_{0.5}\text{O}_3$  perovskite was synthesized by a combined ethylenediaminetetraacetic acid (EDTA)-citric acid complexation method. Total metal ions, EDTA, citric acid, and ammonium hydroxide were preserved at molar ratios of 1:1:2:10 at a fixed precursor molar concentration of 0.05 M. Ammonia aqueous solution was added slowly to a beaker containing EDTA, constantly stirring until the EDTA was entirely dissolved and a clear solution formed. In another beaker, the metal ions and citric acid were dissolved in distilled water for 10 minutes. After that, the EDTA solution was added to the mixed solution while stirring to get the required solution, which then was heated to  $100^\circ\text{C}$  at constant stirring to evaporate most of the water until a viscous fluid formed. The viscous fluid was dried in the oven at  $90^\circ\text{C}$  for 24 hours. The resultant sample was calcinated in the muffle furnace at  $450^\circ\text{C}$  for 8 hours in air at ramping rate of  $5^\circ\text{C min}^{-1}$ . The pre-calcinated sample was further calcinated at  $800^\circ\text{C}$  for 4 hours at ramping rate of  $5^\circ\text{C min}^{-1}$ . The resultant sample was characterized using the X-ray diffraction (XRD, D8 Advance, Bruker, USA) with Cu-Ka ( $\lambda = 1.5406 \text{ \AA}$ ) at 40 kV and 40 mA. The sample was analyzed using Xpert HighScore Software in the range of  $10^\circ \leq 2\theta \leq 60^\circ$  to validate the formation of perovskite phase in resultant catalyst. Electrochemical impedance spectroscopy (EIS) analysis was performed using potentiostat (Autolab PGSTAT204) at a frequency within the frequency range from 1000 kHz to 0.1 Hz using an AC voltage with 5 mV amplitude in order to investigate in-depth understanding on the functional role of bicarbonate in modulating the redox cycle during catalysis in the BAP system.

### 2.3. Oxidative degradation of CBZ in BAP system

The reaction was performed in a 100 ml beaker shaken at a speed of 200 rpm. The reaction mixture was prepared by adding 0.8 g/L  $\text{CaCo}_{0.5}\text{Fe}_{0.5}\text{O}_3$  into 10 mg/L of CBZ solution. Degradation reactions were initiated by adding specified dosage of bicarbonate/ $\text{H}_2\text{O}_2$  ratio ( $R$ ) into the reaction mixture at  $R = 0, 0.5, 1, 5, 10, 15, 20, 25$  and  $\infty$  ( $\text{H}_2\text{O}_2$ : 0 mM,  $\text{NaHCO}_3$ : 44 mM)

to determine the optimum  $R$  value in oxidative degradation of CBZ.  $R$  values can be calculated using Eq. (1).

$$R - \text{value} = \frac{C_{\text{bicarbonate}}}{C_{\text{H}_2\text{O}_2}} \quad (1)$$

where

$C_{\text{bicarbonate}}$  = The concentration of bicarbonate ( $\text{HCO}_3^-$ ),

$C_{\text{H}_2\text{O}_2}$  = The concentration of hydrogen peroxide ( $\text{H}_2\text{O}_2$ ).

The samples were withdrawn and filtered through a 0.45  $\mu\text{m}$  membrane filter at pre-determined time intervals and the ongoing reaction was quenched immediately by adding sodium thiosulphate. Each experiment was conducted in duplicate while the pH remained unadjusted. The supernatant of degraded solution was analyzed using high-performance liquid chromatography (HPLC) at  $\lambda = 285$  nm. The degradation of CBZ was determined using the following Eq. (2):

$$\text{Percentage of CBZ removal (\%)} = \frac{(C_o - C_f)}{C_o} \times 100 \quad (2)$$

Where

$C_o$  = The initial concentration of CBZ,

$C_f$  = The final concentration of CBZ.

### 3. Results and discussion

#### 3.1. Characterization

The phase identification for resultant catalyst was analyzed by XRD analysis as shown in Fig. 1. Detailed summary of analyzed phases is presented in TABLE 1. It was observed that the XRD pattern of sample corresponding to perovskite phases which attributed to  $\text{CaFeO}_3$  (COD 96-152-6750),  $\text{Ca}_2\text{FeO}_5$  (COD 96-152-0831), and  $\text{Ca}_2\text{FeCoO}_5$  (COD 96-400-0921). Meanwhile, impurity phases consist of  $\text{CaO}_2$  (COD 96-153-0293) and  $\text{CoO}_2$  (COD 96-153-1763). Hence, these findings confirm that the re-

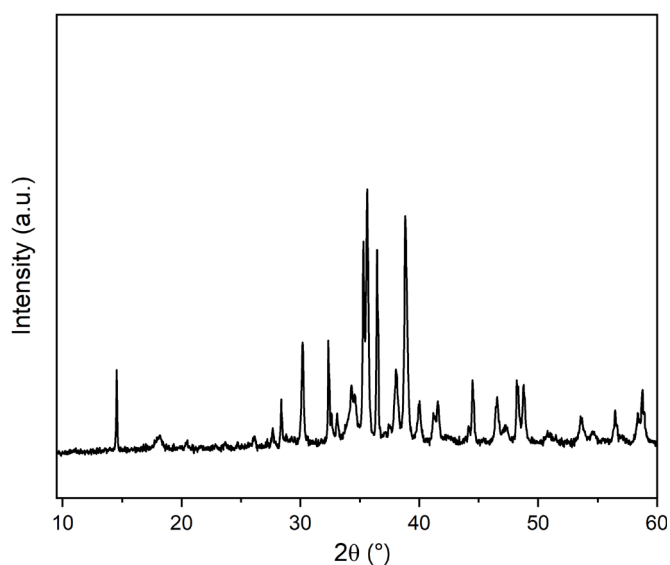


Fig. 1. XRD pattern of  $\text{CaCo}_{0.5}\text{Fe}_{0.5}\text{O}_3$  perovskite catalyst

sultant  $\text{CaCo}_{0.5}\text{Fe}_{0.5}\text{O}_3$  contained mixtures of perovskites (82%) and mixed oxides (18%), as shown in Fig. 1.

TABLE 1

Composition of phase analysis in the  $\text{CaCo}_{0.5}\text{Fe}_{0.5}\text{O}_3$  perovskite catalyst

COD No	Chemical Formula	Phase	Percentage
96-152-6750	$\text{CaFeO}_3$	Perovskite	25%
96-152-0831	$\text{Ca}_2\text{FeO}_5$	Perovskite	19%
96-400-0921	$\text{Ca}_2\text{FeCoO}_5$	Perovskite	38%
96-153-0293	$\text{CaO}_2$	Mixed oxide	17%
96-153-1763	$\text{CoO}_2$	Mixed oxide	1%

#### 3.2. Catalytic performance of BAP- $\text{CaCo}_{0.5}\text{Fe}_{0.5}\text{O}_3$ system

Fig. 2 shows the catalytic performance of the BAP system on CBZ removal in the presence of  $\text{CaCo}_{0.5}\text{Fe}_{0.5}\text{O}_3$  perovskite catalyst at unadjusted pH. The CBZ degradation efficiency is approximately 13% within 45 minutes of reaction time in the absence of bicarbonate ( $R = 0$ ) as a co-oxidant. Meanwhile, the removal rate of CBZ dropped to 10% in the absence of  $\text{H}_2\text{O}_2$  at a fixed 44 mM of bicarbonate ( $R = \infty$ ). Interestingly, the CBZ degradation efficiency improved significantly once the bicarbonate (co-oxidant) was added to the reaction mixture as a BAP system. In the presence of both oxidants at  $R = 20$  (880 mM bicarbonate, 44 mM  $\text{H}_2\text{O}_2$ ), the overall catalytic activity of the oxidation reaction was enhanced by achieving 98% removal of CBZ within 45 minutes. This can be supported by the HPLC chromatogram as presented in Fig. 3. Interestingly, findings of this work (TABLE 2) had surpassed the previous reported works [17,19-22] and comparable to Jawad et al. [16] which showed similar degradation performance of macro-pollutant (99% removal of methyl orange dye) within the same reaction time in the BAP system.

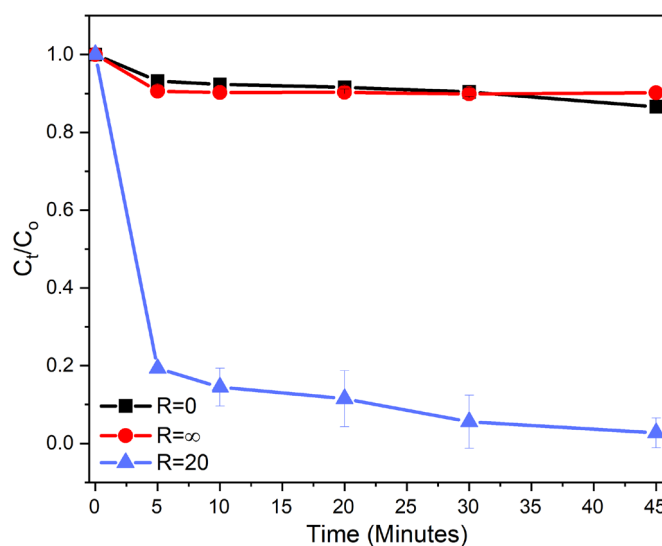


Fig. 2. The CBZ degradation profiles at different dosage of bicarbonate/ $\text{H}_2\text{O}_2$  ratio ( $R$ ). Experimental condition: 10 mg/L CBZ, 44 mM  $\text{H}_2\text{O}_2$ , 0.8 g/L of  $\text{CaCo}_{0.5}\text{Fe}_{0.5}\text{O}_3$  perovskite catalyst, room temperature, and unadjusted pH

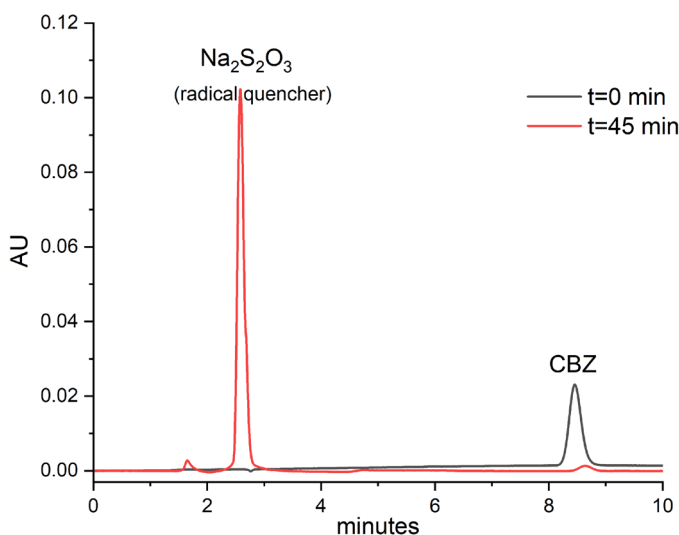


Fig. 3. HPLC chromatogram of CBZ's degradation at  $R = 20$

The increased degradation of CBZ suggests that bicarbonate facilitates the activation of  $\text{H}_2\text{O}_2$  due to the efficient redox cycle of active sites within the structure of perovskite catalyst which subsequently leads to facile generation of reactive radicals ( $\cdot\text{OH}$  and  $\cdot\text{CO}_3^-$ ). Such enhanced redox cycle was attributed to fast charge transfer during catalysis as evidenced by EIS analysis, as shown in Fig. 4. The lowest electron transfer resistance (approximately  $153 \Omega$ ) was found in the presence of both oxidants ( $R = 20$ ). The low resistance leads to faster charge transfer [23] and higher surface reaction rate [24,25] within the surface of  $\text{CaCo}_{0.5}\text{Fe}_{0.5}\text{O}_3$  perovskite catalyst to effectively generate  $\cdot\text{OH}$  and  $\cdot\text{CO}_3^-$  radicals during catalysis.

These findings are consistent with the research conducted by Zhou et al. [26], who reported that the presence of bicar-

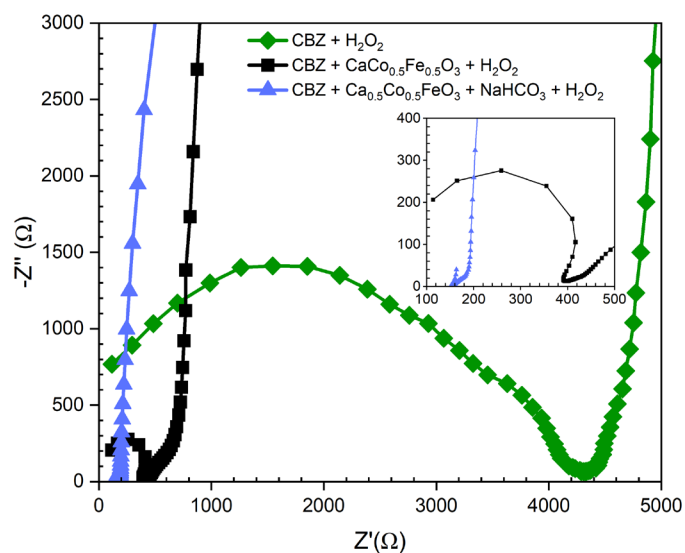


Fig. 4. Nyquist plot of CBZ oxidative degradation in the presence with and without  $\text{CaCo}_{0.5}\text{Fe}_{0.5}\text{O}_3$  perovskite catalyst at single and both oxidants. Experimental conditions: 10 ppm CBZ, 44 mM  $\text{H}_2\text{O}_2$ , 880 mM  $\text{NaHCO}_3$  ( $R = 20$ ), unadjusted pH, and room temperature

bonate resulted in the formation of oxidant active complexes on the catalyst's active sites ( $^{\circ}\text{Co}^{2+}/^{\circ}\text{Co}^{3+}$ ), thereby promoting the generation of reactive radicals ( $\cdot\text{OH}$  and  $\cdot\text{CO}_3^-$ ). The higher formation of these active oxidant complexes during catalysis can enhance the overall catalytic activity of the perovskite catalyst, resulting in improved degradation efficiency. As a result, a synergistic activation of oxidant active complexes to form reactive radicals ( $\cdot\text{OH}$  and  $\cdot\text{CO}_3^-$ ) from  $R = 0$  to  $R = 20$  was observed which subsequently enhances the overall degradation of CBZ.

TABLE 2

Oxidative degradation of organic pollutants in BAP system in presence of heterogeneous catalysts

Catalysts	Model pollutant	Reaction conditions	Percentage of Degradation (%)	References
$\text{CoFeO}_4$	Acid Orange II dye	6 mM $\text{H}_2\text{O}_2$ , 1.19 mM $\text{NaHCO}_3$ , g/L catalyst	20% (45 minutes)	[19]
Diatomite-supported cobalt	Methylene Blue	60 mM $\text{H}_2\text{O}_2$ , 25 mM $\text{NaHCO}_3$ , 1 g/L catalyst	80% (45 minutes)	[20]
Co/Cu/Zeolite	Rhodamine B	20 mM $\text{H}_2\text{O}_2$ , 30 mM $\text{NaHCO}_3$ , 0.2 g/L catalyst	20% (45 minutes)	[21]
Co-Mg-Al Layered Double Hydroxides	4-Chlorophenol	20 Mm $\text{H}_2\text{O}_2$ , 40 mM $\text{NaHCO}_3$ , 1.2 g/L catalyst	70% (1 hour)	[17]
Carbon nanotube	AO7	20 mM $\text{H}_2\text{O}_2$ , 5 mM $\text{NaHCO}_3$ , 0.2 g/L catalyst	20% (40 minutes)	[22]
Co-Mg-Al Layered Double Hydroxides	Methyl Orange	50 mM $\text{H}_2\text{O}_2$ , 25 mM $\text{NaHCO}_3$ , 0.6 g/L catalyst	99% (45 minutes)	[16]
$\text{CaCo}_{0.5}\text{Fe}_{0.5}\text{O}_3$	Carbamazepine	44 mM $\text{H}_2\text{O}_2$ , 880 mM $\text{NaHCO}_3$ , 0.8 g/L catalyst	98% (45 minutes)	Current work

### 3.3. Kinetic model for degradation of CBZ

The degradation profile of the experimental data within 45 minutes of reaction time at the optimum  $R$  value of 20 was fitted to the zero-order, first-order, second-order, and Behnajady-Modirshahla-Ghanbery (BMG) reaction kinetics model, respectively. The BMG kinetic model was adopted to comprehend the limitations of previous models by integrating oxidation capacity into the reaction kinetics [27]. In fact, this model has

been well-adopted to elucidate the reaction kinetic models for oxidative degradation of recalcitrant organic macropollutants, such as acid orange 8 [28], acid red 44 [28], direct blue 71 azo dye [29], reactive yellow 17 [30] and C.I. Acid Yellow 23 [27], particularly in Fenton/Fenton-like reaction processes. The equations of the linear forms of each kinetics model were summarized in TABLE 3.

According to the detailed fittings of each kinetics model as shown in Fig. 5, the BMG kinetics model provide the highest

TABLE 3

Linear forms equation of the zero-order, first-order, second-order, and BMG reaction kinetics

Reaction Order	Zero-order	First order	Second order	BMG model
Differential rate equation	$-\frac{dC_t}{dt} = k_0$	$-\frac{dC_t}{dt} = k_1 C_t$	$-\frac{dC_t}{dt} = k_2 C_t^2$	$\frac{C_t}{C_o} = 1 - \frac{t}{m} + k_b$
Integrated rate equation	$C_t = C_o - k_0 t$	$C_t = C_o e^{-k_1 t}$	$\frac{1}{C_t} = \frac{1}{C_o} + k_2 t$	$\frac{t}{1 - \frac{C_t}{C_o}} = m + k_b t$
Units of Rate Constant	$\text{mg.L}^{-1}.\text{min}^{-1}$	$\text{min}^{-1}$	$\text{L.mg}^{-1}.\text{min}^{-1}$	unitless

Notes:  $C_t$  is the average concentration of CBZ at any time ( $t$ , min),  $C_o$  is the initial concentration of CBZ at time  $t = 0$ ,  $k$  represents the apparent kinetic rate constants of reaction order,  $t$  is the reaction time, and  $k_b$  and  $m$  are two characteristic constants relating to the reaction kinetics and oxidation capacities.

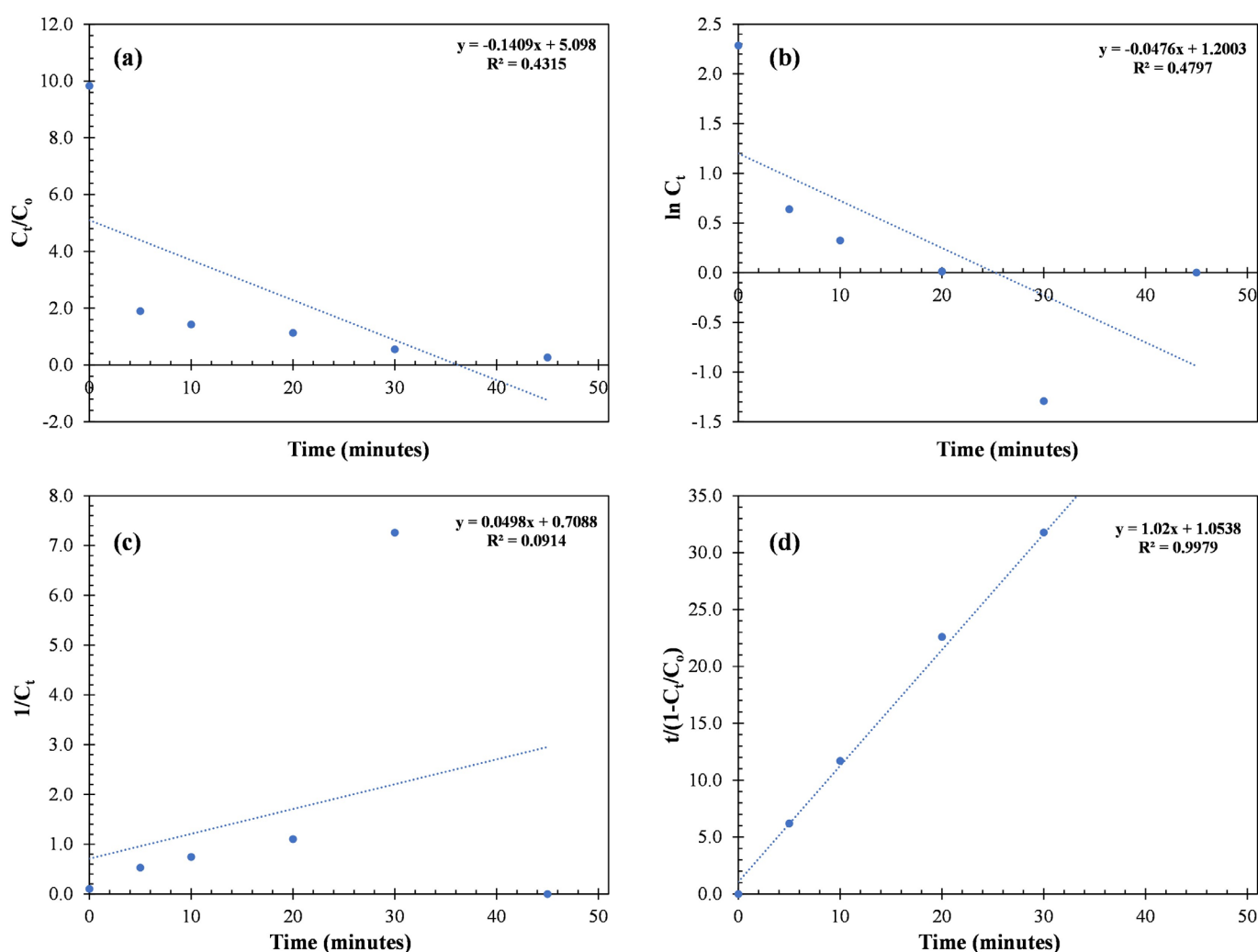


Fig. 5. (a) Zeroth-order, (b) first-order, (c) second-order, and (d) BMG reaction kinetics for the CBZ degradation by Fenton's oxidation within 45 minutes of reaction time ( $R = 20$ , 10 mg/L CBZ, 44 mM  $\text{H}_2\text{O}_2$ , 0.8 g/L of  $\text{CaCo}_{0.5}\text{Fe}_{0.5}\text{O}_3$  perovskite catalyst, room temperature, and unadjusted pH

regression correlation coefficient ( $R^2$ ) of 0.9979 compared to the zero-order (0.4135), first-order (0.4797) and second-order (0.0914) models. Based on these data, the overall catalysis in BAP system can be well represented by the BMG kinetics model. The corresponding parameters involved in this model elucidate the potential activation of  $\text{H}_2\text{O}_2$  by bicarbonate in facilitating  $\text{H}_2\text{O}_2$  activation in the oxidative degradation of CBZ. Such findings corroborate that the BMG kinetics was the optimum kinetics model to describe the oxidative degradation of CBZ in the presence of  $\text{CaCo}_{0.5}\text{Fe}_{0.5}\text{O}_3$  perovskite catalysts in the BAP system.

The BMG reaction kinetics model was further employed to conduct a detailed analysis of the experimental data points derived from the degradation of CBZ at varying  $R$  values ( $R = 0, 0.5, 1, 5, 10, 15, 20, 25, \text{and } \infty$ ) within 45 minutes of reaction time. The reciprocal value of  $k_b$  ( $1/k_b$ ) in BMG reaction kinetics represents the maximum theoretical degradation of CBZ; hence a high degradation rate is favoured at lower  $k_b$ . Fig. 6 shows the maximum oxidation capacity ( $1/k_b$ ) profiling for CBZ degradation using the BMG kinetics model at different  $R$  values. The analysis of the oxidation capacity ( $1/k_b$ ) revealed an exponential increase in the  $1/k_b$  value as  $R$  increased from 0 to 20. At  $R = 20$ , the  $1/k_b$  value reached its highest value of 0.97, indicating a high degradation rate. Based on this data, the oxidation capacity to degrade the CBZ micropollutant improves by nearly 870% in the presence of both oxidants, compared to a single oxidant. However, as  $R$  approached  $\infty$ , the  $1/k_b$  value declines significantly to 0.1. This observation can be attributed to the presence of free  $\text{HCO}_3^-$  molecules in the reaction mixture at higher concentrations, which potentially scavenge  $\cdot\text{OH}$  radicals during catalysis [31]. The scavenging effect reduces the formation of  $\cdot\text{OH}$  radicals and subsequently lowers the degradation efficiency of CBZ. Hence, these results confirmed that the optimum  $R$  was achieved at  $R = 20$ .

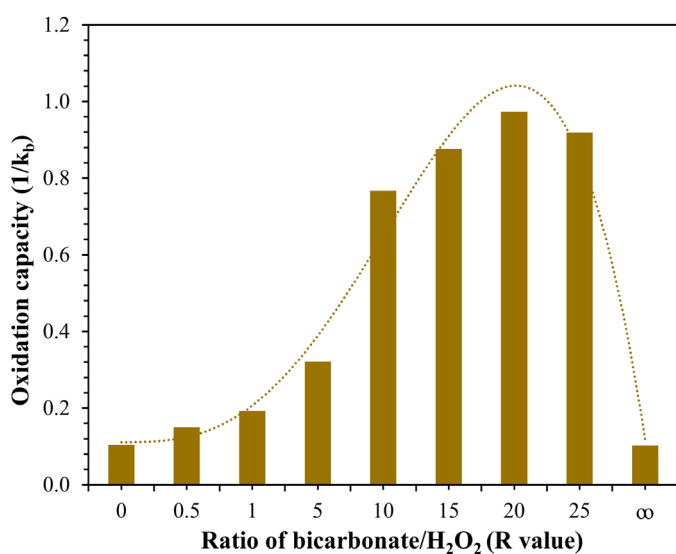


Fig. 6. BMG kinetics for the CBZ degradation at different  $R$  at 45 minutes. Experimental condition: 10 mg/L CBZ, 44 mM  $\text{H}_2\text{O}_2$ , 0.8 g/L of  $\text{CaCo}_{0.5}\text{Fe}_{0.5}\text{O}_3$  perovskite catalyst, room temperature, and unadjusted pH

#### 4. Conclusion

In summary, this study confirms the synergistic role of bicarbonate as co-oxidant towards facile activation of  $\text{H}_2\text{O}_2$  into the efficient generation of reactive radicals in the presence of  $\text{CaCo}_{0.5}\text{Fe}_{0.5}\text{O}_3$  perovskite catalyst during oxidative degradation of CBZ. At the optimum dosage of  $R = 20$  (880 mM bicarbonate, 44 mM  $\text{H}_2\text{O}_2$ ), an almost complete degradation up to 98% was achieved within 45 minutes of reaction time. These results show a significant improvement over the use of either  $\text{H}_2\text{O}_2$  or bicarbonate alone (10-13%) under comparable conditions. The improved overall catalytic performance was attributed to efficient redox cycle of catalysts' active sites in presence of both oxidants to effectively generate higher reactive radicals ( $\cdot\text{OH}$  and  $\cdot\text{CO}_3^-$ ) in degrading CBZ during catalysis. The oxidative degradation of CBZ in the presence of BAP- $\text{CaCo}_{0.5}\text{Fe}_{0.5}\text{O}_3$  system is well-fitted to a BMG reaction kinetics model. The model shows a progressive increase trend in the oxidation capacity ( $1/k_b$ ) from  $R = 0$  to the highest value of 0.97 at  $R = 20$ , indicating the highest degradation capacity compared to other  $R$  values. However, despite the promising results of this study, further investigations are warranted as this work is still at the fundamental phase. For instance, the leaching and analysis of the intermediate by-products need to be confirmed to ensure the safety of BAP- $\text{CaCo}_{0.5}\text{Fe}_{0.5}\text{O}_3$  system for large-scale applications. These tests help to assess the possible release of intermediates or undesirable substances from the reaction system as to ensure that the quality of the treated water is safe and complies with the regulatory standards and guidelines for water treatment.

#### Acknowledgement

The authors would like to acknowledge the Ministry of Higher Education Malaysia (MOHE) and Universiti Teknologi MARA Cawangan Pulau Pinang for the financial support under Fundamental Research Grant Scheme (FRGS/1/2023/TK09/UITM/02/22) and the Sydney Southeast Asia Centre for the Collaborative Research Grant (100-TNCPI/INT 16/6/2 (006/2022)).

#### REFERENCES

- [1] J.L. Wilkinson, A.B.A. Boxall, D.W. Kolpin et al., Pharmaceutical pollution of the world's rivers. *Proceedings of the National Academy of Science of the United States of America* **119** (8), 2113947119 (2022).
- [2] H. Khazri, S. Ben Hassine, I. Ghorbel-Abid et al., Presence of carbamazepine, naproxen, and ibuprofen in wastewater from northern Tunisia. *Environmental Forensics* (20), 121-128 (2019).
- [3] NORMAN, NORMAN Database System. <https://www.norman-network.com/nds/common/2005> (accessed April 22, 2024).
- [4] B. Wooge, U.S. EPA Endocrine Disruptor Screening Program Comprehensive Management Plan. <https://www.epa.gov/sites/default/files/2014-03/000012main.pdf>

- fault/files/2015-08/documents/edsp-comprehensive-management-plan-2012.pdf, 2012 (accessed April 22, 2024).
- [5] N.S.P. Batucan, L.A. Tremblay, G.L. Northcott et al., Medicating the environment? A critical review on the risks of carbamazepine, diclofenac and ibuprofen to aquatic organisms. *Environmental Advances* **7**, 100164 (2022).
- [6] P. Bhatt, G. Bhandari, M. Bilal, Occurrence, toxicity impacts and mitigation of emerging micropollutants in the aquatic environments: Recent tendencies and perspectives. *Journal of Environmental Chemical Engineering* **10**, 3, 107598 (2022).
- [7] C. Fernández-López, J.M. Guillén-Navarro, J.J. Padilla et al., Comparison of the removal efficiencies of selected pharmaceuticals in wastewater treatment plants in the region of Murcia, Spain, *Ecological Engineering* **95**, 811-816 (2016).
- [8] F.I. Hai, S. Yang, M.B. Asif et al., Carbamazepine as a Possible Anthropogenic Marker in Water: Occurrences, Toxicological Effects, Regulations and Removal by Wastewater Treatment Technologies. *Water* **10**, 107 (2018).
- [9] A.K. Thakur, R. Kumar, A. Kumar et al., Pharmaceutical waste-water treatment via advanced oxidation based integrated processes: An engineering and economic perspective, *Journal of Water Process Engineering* **54**, 103977 (2023).
- [10] S. Feijoo, M. Kamali, R. Dewil, A review of wastewater treatment technologies for the degradation of pharmaceutically active compounds: Carbamazepine as a case study, *Chemical Engineering Journal* **455**, 140589 (2023).
- [11] C.M. Dai, X.F. Zhou, Y.L. Zhang et al., Comparative study of the degradation of carbamazepine in water by advanced oxidation processes, *Environmental Technology* **33**, 1101-1109 (2012).
- [12] G. Sönmez, T. Bahadır, M. Işık, Removal of selected pharmaceuticals from tap water by the Fenton process. *International Journal of Environmental Analytical Chemistry* **102** (16), 3855-3867 (2022).
- [13] J. Deng, Y. Shao, N. Gao et al., Degradation of the antiepileptic drug carbamazepine upon different UV-based advanced oxidation processes in water. *Chemical Engineering Journal* **222**, 150-158 (2013).
- [14] J. Wang, S. Li, Q. Qin et al., Sustainable and feasible reagent-free electro-Fenton via sequential dual-cathode electrocatalysis. *Proceedings of the National Academy of Sciences of the United States of America* **118**, 2108573118 (2021).
- [15] H. Pan, Y. Gao, N. Li et al., Recent advances in bicarbonate-activated hydrogen peroxide system for water treatment. *Chemical Engineering Journal* **408**, 127332 (2021).
- [16] A. Jawad, Y. Li, X. Lu et al., Controlled leaching with prolonged activity for Co-LDH supported catalyst during treatment of organic dyes using bicarbonate activation of hydrogen peroxide. *Journal of Hazardous Materials* **289**, 165-173 (2015).
- [17] A. Jawad, Y. Li, X. Lu et al., Degradation of chlorophenols by supported Co-Mg-Al layered double hydroxide with bicarbonate activated hydrogen peroxide. *Journal of Physical Chemistry A* **118**, 10028-10035 (2014).
- [18] J. Jing, M.N. Pervez, P. Sun et al., Highly efficient removal of bisphenol A by a novel Co-doped LaFeO<sub>3</sub> perovskite/PMS system in salinity water. *Science of the Total Environment* **801**, 149490 (2021).
- [19] X. Guo, H. Li, S. Zhao, Fast degradation of Acid Orange II by bicarbonate-activated hydrogen peroxide with a magnetic S-modified CoFe<sub>2</sub>O<sub>4</sub> catalyst. *Journal of the Taiwan Institute of Chemical Engineers* **55**, 90-100 (2015).
- [20] L. Zhou, W. Song, Z. Chen et al., Degradation of Organic Pollutants in Wastewater by Bicarbonate-Activated Hydrogen Peroxide with a Supported Cobalt Catalyst. *Environmental Science and Technology* **47**, 3833-3839 (2013).
- [21] X. Zhang, D. Ma, X. Zhu, Insights into bicarbonate enhanced heterogeneous Fenton catalyzed by Co/Cu/zeolite for degradation of rhodamine B. *Environmental Engineering Research* **29**, 230095 (2024).
- [22] H. Dong, X. Feng, Y. Guo et al., Bicarbonate activated hydrogen peroxide with cobalt nanoparticles embedded in nitrogen-doped carbon nanotubes for highly efficient organic dye degradation. *Colloids and Surfaces A: Physicochemical and Engineering Aspects* **630**, 127645 (2021).
- [23] C. Su, X. Duan, J. Miao et al., Mixed Conducting Perovskite Materials as Superior Catalysts for Fast Aqueous-Phase Advanced Oxidation: A Mechanistic Study. *ACS Catalysis* **7**, 388-397 (2017).
- [24] M. Gao, W. Sheng, Z. Zhuang et al., Efficient water oxidation using nanostructured  $\alpha$ -nickel-hydroxide as an electrocatalyst. *Journal of American Chemical Society* **136**, 7077-7084 (2014).
- [25] P. Gao, X. Tian, W. Fu et al., Copper in LaMnO<sub>3</sub> to promote peroxy monosulfate activation by regulating the reactive oxygen species in sulfamethoxazole degradation. *Journal of Hazardous Materials* **411**, 125163 (2021).
- [26] X. Du, M. Zhou, Strategies to enhance catalytic performance of metal-organic frameworks in sulfate radical-based advanced oxidation processes for organic pollutants removal. *Chemical Engineering Journal* **403**, 126346 (2021).
- [27] M.A. Behnajady, N. Modirshahla, F. Ghanbary, A kinetic model for the decolorization of C.I. acid yellow 23 by Fenton process. *Journal of Hazardous Materials* **148**, 98-102 (2007).
- [28] S. Tuncı, O. Duman, T. Gürkan, Monitoring the decolorization of acid orange 8 and acid red 44 from aqueous solution using Fenton's reagents by online spectrophotometric method: Effect of operation parameters and kinetic study. *Industrial and Engineering Chemistry Research* **52**, 1414-1425 (2013).
- [29] N. Ertugay, F.N. Acar, Removal of COD and color from direct blue 71 azo dye wastewater by Fenton's oxidation: Kinetic study. *Arabian Journal of Chemistry* **10**, S1158-S1163 (2017).
- [30] N. Bougdour, A. Sennaoui, I. Bakas et al., Experimental evaluation of reactive yellow 17 degradation using UV light and iron ions activated peroxydisulfate: Efficiency and kinetic model. *Science and Technology of Materials* **30**, 157-165 (2018).
- [31] L. Duan, Y. Chen, K. Zhang et al., Catalytic degradation of acid orange 7 with hydrogen peroxide using Co<sub>x</sub>O<sub>y</sub>-N/GAC catalysts in a bicarbonate aqueous solution. *Royal Society of Chemistry* **5**, 84303-84310 (2015).